Article:
Rahimi, Zahra, Ghanbari, Reza, Mohajerzadeh, Amirhossein et al. (1 more author) (2024) 3D UAV Small Cell Base Station Positioning and Resource Allocation in Cellular Network:A Stochastic Optimization Approach. IEEE Internet of Things Journal. pp. 10951-10963. ISSN: 2327-4662

https://doi.org/10.1109/JIOT.2023.3329718

3D UAV Small Cell Base Station Positioning and Resource Allocation in Cellular Network: A Stochastic Optimization Approach

Zahra Rahimi, Reza Ghanbari, Amir Hossein Mohajerzadeh, and Hamed Ahmadi

***Abstract*—Integrating Unmanned Aerial Vehicles (UAVs) into wireless communication as aerial platforms to mount small cell base stations has grown rapidly in recent years. One of the main objectives of UAV integration into wireless networks is to optimize UAV deployment while meeting user expectations with the fewest UAVs. To ensure that users receive the requested data rate, management of UAV placement and user association is necessary due to the limited capacity of aerial base stations. Besides the user-base station distance, environmental conditions and propagation mode affect the data rate received by the users. When accounting for uncertain conditions, network management decisions become more realistic and productive. This paper considers a random propagation mode for each link depending on the environmental conditions of the desired area. We exploit the stochastic programming framework to reflect propagation mode uncertainty in the optimization problem, which impacts the received data rate and path loss. The suggested mathematical formulation determines the minimum number of required UAVs, their 3D positions, and the best user association strategy. The proposed model also includes interference-aware constraints for optimal radio resource allocation to base stations. The nonlinear path loss and LoS probability distribution functions in terms of the base station positions lead to a non-linear formulation. We obtain a mixed-binary linear formulation by replacing non-linear functions with their piecewise linear approximations and solve the model accurately using the CPLEX solver. The implementation results show that stochastic approaches provide more accurate diagnoses of the environment, as well as superior performance to deterministic optimization.**

***Index Terms*—Stochastic programming, UAV positioning, Channel assignment, Probability of LoS propagation**

I. Introduction

The rapid growth of applications and mobile devices makes future cellular communications face the scarcity of spectrum bands challenge. Currently, cell densification is a promising solution to deal with the 5G wireless network's enormous surge in data traffic. Adding more cell sites can significantly expand network coverage and capacity, especially in regions traditionally difficult to penetrate [1]. Nonetheless, there are many limitations to the excessive deployment of traditional terrestrial networks. As an example, deploying ground infrastructure is not affordable and practical for temporary events (e.g. concerts and sports events) or Radio Access Network (RAN) congestion scenarios (e.g. hotspot regions during rush hour). In these cases, the versatility and mobility of unmanned aerial vehicles (UAVs) equipped by small cells make them a good choice for establishing aerial base stations to provide users with more reliable real-time and on-demand communication [2].

Zahra Rahimi and Reza Ghanbari are with Ferdowsi University of Mashhad, Mashhad, Iran, (e-mail: rahimi.zahra@mail.um.ac.ir; rghanbari@um.ac.ir).

Amirhossein Mohajerzadeh is with the Sohar University, Sohar, Oman, (e-mail: amirhossein@su.edu.om).

Hamed Ahmadi is with the University of York, UK, (e-mail: hamed.ahmadi@york.ac.uk).

Due to the limited resource capacity of a single UAV network, a multi UAVs network is a promising solution for various missions. However, the integration of multiple UAV base stations (UAV-BSs) into wireless networks poses several challenges, such as resource management, positioning, and channel modeling [3]. Clearly, practical solutions cannot be found by addressing these issues separately without considering their interactions. For instance, high-altitude of UAVs can vary the channel condition and increase the line of sight probability while reducing the coverage due to high co-channel interference and rising path loss [4]. Furthermore, the distance between BSs can influence the way the frequency band should be distributed. An inefficient resource allocation strategy may leads to inter-cell interference, which in turn affects user transmit power and throughput [5]. These challenges become more complicated under financial considerations and the uncertainty caused by environmental characteristics.

As the UAV position plays a crucial role in network performance, a large and growing body of literature on UAV-assisted cellular communication has highlighted the optimal UAV placement issue. These studies have been coverd a variety of objectives including maximum coverage [6] - [10], maximum throughput [11] - [14], energy efficiency [9], [15] - [17], etc. However, the fluid arrangement of UAV-BSs and the possibility of overlap between their coverage areas make interference a common problem in multiple UAV deployments. An investigation of interference effects in a UAV-based network is presented in [18]. The authors in [18] calculate the optimal distance between two interfering UAVs flying at a fixed altitude to maximize coverage area. Using the SINR metric, [19] studies the effect of BSs' position on the coverage area optimization in the presence of co-channel interference in two scenarios of symmetric and asymmetric BS placement. A considerable amount of literature have studied interference-aware UAV positioning to eliminate any potential challenges caused by interfering BSs [20], [21], [22], [23]. These studies have attempted to deploy UAVs avoiding overlap between BSs' coverage areas. In a relay positioning research, [20] proposes a genetic interference-aware technique to increase downlink throughput. With the aim of maximizing users' coverage probabilities, [21] groups users into non-overlapping elliptical regions to prevent inter-cell interference. In [22], circle packing theory is employed for maximizing coverage performance. Using K -means clustering method [23] divides the target area into K convex subareas and, in a step-by-step manner, finds the optimal location of UAVs, which ensures that the next UAV always deploys in a position that avoids inter-cell interference. Although this clustering decreases interference, the users' satisfaction rate is also degraded because their requirements are not taken into account. Coordinated multipoint (CoMP) algorithms are used in [24] and [25] where the users are divided into several groups and orthogonal bandwidth are used to serve different groups. This resource allocation scheme

results in a lower frequency reuse ratio, which can reduce long term network throughput.

Cellular networks can utilize frequency reuse approach to handle large numbers of cells with a limited number of channels. As each cell uses radio frequencies only within its boundaries, in cells with no overlapped coverage areas, radio frequencies can be reused. To date, several studies introduced frequency reuse techniques to mitigate intracell and intercell interferences when sharing frequency resources in wireless networks [26], [27], [28]. According to [26], strict fractional frequency reuse (FFR) partitions a cell area into spatial regions with different frequency reuse factors, while soft frequency reuse (SFR) divides a cell area into two regions: an inner region with all of the frequency resources and an outer region with only a fraction of the resources. Although SFR can be more bandwidth-efficient than strict FFR, this approach leads to more intercell interference for both edge and cell-interior users. As strict FFR does not share any frequencies, it reduces interference between cell-interior and cell-edge users. A flexible SFR (F-SFR) technique has been proposed in [27] to accommodate flying BSs by assigning frequency resource plans that take into account the dynamic network topology. The authors of [27] maximize the inter-BS distance among cells with the same resource plan by varying the SFR levels in each cell. In [28] the optimal frequency reuse factor is found by a hierarchical multi-agent reinforcement learning framework to maximize the energy efficiency of UAVs.

An interference management strategy along with a BS placement that meets users' requirements depends on the propagation environment. Depending on the propagation model, UAV arrangements may differ based on the path loss experienced by the users. Since the propagation condition is not specified before UAV deployment, in most studies, fixed propagation conditions have been assumed, or the expected value of path loss based on LoS and NLoS propagations has been considered in computations. A recent study by Nguyen et al. [29] has attempted to quantify the impact of all propagation configurations on UAV placement and resource allocation. However, path loss was included as an expected value in the formulation developed by [29]. Using averaging to account for uncertainty in propagation conditions and path loss results in considering all possible scenarios influencing the final decision. Nonetheless, in this approach, the entire probability distribution of the uncertain parameter is collapsed to a one-point. While in many cases, the realization of an uncertain parameter does not correspond to its expected value. In [30], the authors investigate how different blockage environments and UAV altitude can influence the outage probability of a link between a UAV and a terrestrial base station, and then, they formulate connectivity outage constraint as a constrained Markov Decision Process for UAV path design [31]. Our previous work proposed a stochastic programming framework to establish an optimum UAV placement scheme under uncertain conditions [32]. The presented model considers a maximum threshold of path loss for all potential communication links. This is while the upper bound of allowed path loss to ensure satisfying each user demand should be regarded based on the data rate required by the user. In addition, [32] does not account for the interference influences on the data rate received by users.

In this paper, we consider a cellular network where a terrestrial BS and UAV-BSs collaborate to construct a network for serving users in a temporary situation when the ground BS cannot cover all users in congestion scenarios, or when other ground BSs break down due to bad weather conditions, vandalism, transmission failure, etc. To exploit the UAVs in a cost-effective manner, we simultaneously minimize the number of required UAVs and optimize their 3D location. The proposed formulation also includes frequency reuse constraint to avoid any intercell interference between UAVs. In order to satisfy users' data rate requirements, our computations take path loss into account as the main component of attenuation. Three commonly used stochastic optimization strategies are used to deal with uncertainty in propagation and the equivalent deterministic models are presented for each one. Due to the nonlinear relations between path loss and probability distribution of LoS communication with the location of BSs, the resulting mathematical models are nonlinear in terms of decision variables. We use piecewise linear approximations of nonlinear functions to obtain mixed-binary linear formulations. To sum up, the main contribution of this work are as follows:

- To minimize the number of required UAV, we propose a mathematical optimization model that finds the optimal 3D deployment of UAV-BSs, user association, and channel assignment.
- Considering the propagation model as a stochastic parameter, we formulate the path loss limits for providing the data rate required as stochastic constraints.
- We apply novel formulations of the Worst Case, Expected Value, and Chance Constrained strategies to achieve deterministic mathematical models with real-world use cases.
- To linearize the mathematical model, we employ piecewise linear approximations of the path loss and propagation distribution functions.
- To lower the computational complexity, we solve the problem in two stages, the first for optimizing UAV placement and user association and then the channel sets are optimized.

The rest of this paper is organize as follows. In Section II the system model of the problem is presented. Section III focuses on the problem formulation. In Section IV we introduce strategies to deal with uncertainty in propagation conditions. Section V provided the approximations of the nonlinear constraints. Section VI presented model decomposition method and in Section VII numerical results are reported.

II. System model

We concentrate on a cellular network that uses small cells mounted on UAVs as aerial BSs to improve the coverage for a set of ground users (J) in an area with a single terrestrial infrastructure (e.g., a disaster zone). We assume that the location and demanded data rate of users (DR_j), the capacity of the ground BS (D_T) and the capacity considered for each small cell (D) are given. The small cells' data rate should be distributed among users in such a way that each BS can accommodate the demands of the users within their coverage area.

The primary goal of this paper is to integrate as few UAVs as possible into the network, to enhance coverage and serviceability by efficiently exploiting radio resources. It is important to ensure that minimizing the number of aerial BSs does not result in low quality of service. In this way, any inter-cell and intra-cell interference should be avoided in UAV deployment and frequency allocation. In addition, by taking path loss into account as the main attenuation factor, small cell placement, user association, and channel assignment must be done in a way to meet the data rates required by the users. Path loss is primarily determined by the distance between the receiver and the BS. There are, however, minor factors that affect the amount of path loss that user experiences, such as environmental characteristics and undetermined propagation modes. So, we are facing a programming problem under

uncertain conditions. We will present the problem formulation below in more detail.

III. Problem Formulation

Here, we assume that a set of potential candidates for the projection of UAVs' positions in the ground (I) is given. The presented formulation takes the set I and chooses a minimum number of points among this set to cover at least α percent of the users. To detect the selection of a point, we define a binary decision variable m_i that takes the value of 1 if the ith candidate point is selected as a UAV position and 0 otherwise. So, in addition to the selection status, the UAV altitude must be optimized based on the coverage target and the minimum data rate required by the users. Our formulation includes a continuous decision variable h_i for the altitude of UAV deployed in ith candidate point. The mathematical model must value the h_i variables in such a way that h_i for the selected candidate point belongs to the allowable flying altitude range $([H_{min}, H_{max}])$ while ensuring the required data rate by the users are met.

TABLE I: Deterministic parameters.

Parameters	Description
f_c	Carrier frequency
C	Speed of light
I	Set of candidate points
J	Set of users
D	Total data rate of UAV-BS
D_T	Total data rate of terrestrial BS
U	Number of users
R_T	Coverage radius of the terrestrial BS
α	Minimum percentage of requested coverage
$H_{\min}$	Minimum allowed altitude
$H_{\max}$	Maximum allowed altitude
θ	UAV coverage angle
DR_j	Data rate required for user j
d_{ij}	Horizontal euclidean distance between user j and candidate point i
d_{Tj}	Horizontal euclidean distance between user j and the terrestrial BS
M	A big number

As we mentioned in system model, we assume that a single ground BS operates in the target area. To determine whether user j is served by the terrestrial BS, the formulation contains a binary decision variable y_j. Small cells carried by UAVs should be used to serve users who are not covered by the terrestrial BS. To identify the links between users and UAV-BSs, the binary variable x_{ij} is employed. x_{ij} is 1, if user j is assigned to the UAV deployed at candidate point i, and 0 otherwise. Following the definition of the decision variables and given parameters provided in Table I and III, the objective function and the basic constraints of candidate point selection and user association are as follows:

TABLE II: Decision variables

Parameters	Description
m_i	1, if candidate point i is selected for UAV deploying, and 0, otherwise.
h_i	The altitude of UAV is deployed at the candidate point i and 0, otherwise
y_j	1, if user j is served by terrestrial BS, and 0, otherwise.
x_{ij}	1, if user j is served by UAV deployed at candidate point i, and 0, otherwise.

$$\min \sum_{i\in I} m_i \tag{1a}$$

s.t

$$y_j + \sum_{i\in I} x_{ij} \le 1, \quad \forall j \in J, \tag{1b}$$

$$\sum_{j\in J} x_{ij} \le U \times m_i, \quad \forall i \in I, \tag{1c}$$

$$\sum_{i\in I}\sum_{j\in J} x_{ij} + \sum_{j\in J} y_j \ge \alpha \times U, \tag{1d}$$

$$\sum_{j\in J} DR_j \times x_{ij} \le D, \quad \forall i \in I, \tag{1e}$$

$$\sum_{j\in J} DR_j \times y_j \le D_T, \tag{1f}$$

$$h_i \ge H_{\min}, \quad \forall i \in I, \tag{1g}$$

$$y_j \le \frac{R_T}{d_{Tj}}, \quad \forall j \in J, \tag{1h}$$

$$x_{ij} \times \cot(\theta) \le \frac{h_i}{d_{ij}}, \quad \forall i \in I, \forall j \in J, \tag{1i}$$

The objective function (1a) is defined to minimize the number of deployed UAVs. Constraint (1b) states that each user can only get service from one BS. Constraint (1c) states that if no UAVs are deployed at the candidate point i, no user can be assigned to it. Constraint (1d) guarantees at least α percent coverage of users. Constraint (1e) and (1f) allow each BS to serve as high a data rate as it can. Constraint (1g) states that UAVs must maintain a minimum flight altitude. Constraints (1h) and (1i) prevent users outside the BS coverage range from being assigned to them. In these limitations, R_T is the coverage radius of the terrestrial BS, d_{Tj} is its distance from user j, d_{ij} is the distance between user j and candidate point i, and θ is the UAV coverage angle. When the distance between user j and the ground BS exceeds the coverage radius, $\frac{R_T}{d_{Tj}}$ will be less than 1. Consequently, constraint (1h) activates and the binary variable y_j is set to 0. Similarly, for assigning user j to UAV-BS i, constraint (1i) is decisive. In this scenario, it should be noticed that the UAV's coverage radius is $h_i \times \tan(\theta)$. To confirm the validity of constraint (1i), please refer to Lemma 1 of [33].

A. User association

Inequalities (1c)-(1i) represent the technical limitations of BSs on user association, including the coverage area and the maximum data rate each can serve. Nonetheless, other factors such as interference and maximum path loss need to be managed to ensure that the requested data rate can be delivered. Here, we present path loss management constraints, and in the next part, we will offer interference-aware constraints on radio resource assignment to prevent interference in communication.

According to Shannon-Hartley theorem, the maximum rate at which information can be transmitted over a communications channel of a specified bandwidth (β) in the presence of noise is equal to $\beta \times \log_2(1 + SNR_{ij})$ or approximately $0.332 \times \beta \times SNR_{ij}^{(dB)}$. Therefore, UAV placement and user association strategy must ensure that users' requested data rates are not more than the maximum rate over their communication channel with the associated BS. To achieve the equivalent mathematical expression of this requirement for user j and the UAV-BS located at candidate point i, we rely on the defined parameters listed in Table III.

Meeting the data rate demanded by users can be restated as follows:

$$0.332 \times \beta \times SNR_{ij}^{(dB)} \ge DR_j, \tag{2}$$

TABLE III: User association parameters

Parameters	Description
β	Bandwidth of communication channel
p_t	Transmitted power
p_T	Transmitted power of terrestrial BS
p_n	Noise power
h_T	Altitude of the terrestrial BS
f_c	Carrier frequency
c	Speed of light
ξ	Uncertain parameter indicates the propagation mode LoS or NLoS
η_ξ	Excessive path loss coeficient for propagation mode ξ

which results in

$$SNR_{ij}^{(dB)} \geq \frac{1}{0.332}\frac{DR_j}{\beta}. \tag{3}$$

SNR is a metric used to compare the level of the intended signal to the background noise level:

$$SNR = \frac{\text{recieved power}}{\text{noise power}}, \tag{4}$$

which in terms of channel gain (G) is stated as follows:

$$SNR = \frac{G \times p_t}{p_n} \tag{5}$$

As the path loss is the inverse of channel gain $(PL = \frac{1}{G})$, we have:

$$\begin{aligned} SNR_{ij}^{(dB)} &= 10\log_{10}(\frac{p_t}{PL_{ij} \times p_n}) \\ &= 10\log_{10} p_t - 10\log_{10} p_n - 10\log_{10} PL_{ij} \\ &= p_t^{(dB)} - p_n^{(dB)} - PL_{ij}^{(dB)} \end{aligned} \tag{6}$$

As a consequence of (3) and (6), we have:

$$PL_{ij}^{(dB)} \leq p_t^{(dB)} - p_n^{(dB)} - \frac{1}{0.332}\frac{DR_j}{\beta}. \tag{7}$$

The inequality (7) must hold if user j is assigned to UAV i, and otherwise can be relaxed. This requirement is met by constraint (8).

$$PL_{ij}^{\xi(dB)} \leq p_t^{(dB)} - p_n^{(dB)} - \frac{1}{0.332}\frac{DR_j}{\beta} + (1-x_{ij})M \quad \forall i \in I, \forall j \in J, \tag{8}$$

where $PL_{ij}^{\xi(dB)}$ is the path loss between UAV deployed at candidate point i and user j. In the same way, the terrestrial BS user assignment constraint must be met:

$$PL_{Tj}^{\xi(dB)} \leq p_T^{(dB)} - p_n^{(dB)} - \frac{1}{0.332}\frac{DR_j}{\beta} + (1-y_j)M \quad \forall j \in J \tag{9}$$

Here, $PL_{Tj}^{\xi(dB)}$ represents the path loss between ground BS and user j. The path loss functions in constraints (8) and (9) are defined as follows:

$$PL_{ij}^{\xi(dB)} = \eta_\xi + FSPL_{ij} \quad \xi \in \{LoS, NLoS\} \tag{10}$$

$$PL_{Tj}^{\xi(dB)} = \eta_\xi + FSPL_{Tj} \quad \xi \in \{LoS, NLoS\}. \tag{11}$$

where $FSPL$ refers to free space path loss and is calculated as follows:

$$FSPL_{ij} = 20\log_{10}(\frac{4\pi f_c}{c}) + 20\log_{10}(\sqrt{d_{ij}^2 + h_i^2}) \tag{12}$$

$$FSPL_{Tj} = 20\log_{10}(\frac{4\pi f_c}{c}) + 20\log_{10}(\sqrt{d_{Tj}^2 + h_T^2}) \tag{13}$$

As stated in constraints (8) - (11), the propagation condition ξ (LoS or NLoS) influences user association strategies and UAV placement. Propagation mode is a random parameter for a given communication channel having a distribution functions of (14) and (15) for A2G links and (16) and (17) for G2G ones.

$$\mathbb{P}_{ij}[\xi = LoS] = \frac{1}{1 + ae^{-b(\arctan(\frac{h_i}{d_{ij}}) - a)}} \tag{14}$$

$$\mathbb{P}_{ij}[\xi = NLoS] = 1 - \mathbb{P}_{ij}[\xi = LoS] \tag{15}$$

$$\mathbb{P}_{Tj}[\xi = LoS] = min\{1, \frac{k_0}{d_{Tj}}\}(1 - e^{-\frac{d_{Tj}}{k_1}}) + e^{-\frac{d_{Tj}}{k_1}} \tag{16}$$

$$\mathbb{P}_{Tj}[\xi = NLoS] = 1 - \mathbb{P}_{Tj}[\xi = LoS] \tag{17}$$

In above distribution functions a and b depend on the environment, e.g., height and density of buildings, urban or sub-urban areas, etc. Also, the parameters k_0 and k_1 characterize the LoS and NLoS critical distances respectively. Since the propagation mode is not specified before decision-making and establishing communications, these constraints deal with non-deterministic parameters. In section IV, we will present strategies to tackle uncertainty in the data.

B. Channel assignment

In this paper, we aim to provide strategies for UAV placement and radio resource allocation in which any inter-cell and intra-cell interference is prevented. To do so, we divide the frequency band into several channel groups, each containing orthogonal frequencies, and no two sets have channels in common. Radio resources are allocated to BSs by assigning a set of channels to each one. Due to the orthogonal frequencies in each set, no intra-cell interference occurs. As there might be fewer channel sets than BSs, some should be assigned to more than one BS. The resource allocation proposed in this paper prevent inter-cell interference by ensuring that the same channel group is not assigned to UAVs with overlapped coverage areas. The overlapped UAVs can be identified using the following lemma.

Lemma 1. *Suppose that two UAVs are deployed at candidate points i and i' that are distant by $D_{ii'}$. Also assume that the UAVs have altitudes of h_i and $h_{i'}$, respectively, and a coverage angle of θ. The coverage areas of the two UAVs overlap if and only if $(h_i + h_{i'})\tan(\theta) > D_{ii'}$.*

Proof. According to Figure 1, the coverage radius of a UAV deployed at altitude h_i with a coverage angle of θ is $R_i = h_i\tan(\theta)$. So we have:

The coverage areas of UAVs overlap $\Leftrightarrow$
The positions of UAVs are projected on the ground at a distance less than the sum of their coverage radius. $\Leftrightarrow$
$D_{ii'} < (h_i + h_{i'})\tan(\theta)$.

□

To prevent inter-cell interference between the two selected candidate points, the altitude of the UAVs and the channel assignment must be configured so that the same channel set

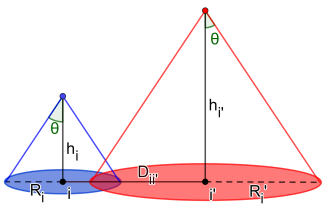

(a) Overlapped coverage areas

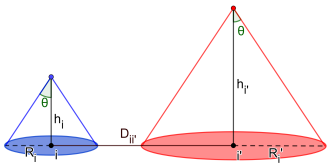

(b) Non-overlapped coverage areas

Fig. 1: UAV coverage

is not assigned to the UAVs in case of overlapped coverage areas. We formulate this requirement as follows:

$$\sum_{p\in P} s_{ip} \geq m_i \quad \forall i \in I, \tag{18a}$$

$$s_{ip} + s_{i'p} \leq 1 + \frac{M - ((h_i + h_{i'})\tan(\theta))}{M - D_{ii'}} \quad \forall i, i' \in I \quad \forall p \in P, \tag{18b}$$

$$|I| \times e_p \geq \sum_{i\in I} s_{ip} \quad \forall p \in P, \tag{18c}$$

where M is a big constant, and P is a collection of channel sets. The binary decision variable e_p indicates whether the channel set p is used or not. Assigning the channel set p to the UAV deployed at candidate point i is determined by the binary variable s_{ip}. Constraint (18a) states that a channel set must be assigned to each selected candidate point. In constraint (18b), if the coverage areas of UAV i and i' overlap ($(h_i + h_{i'})\tan(\theta) > D_{ii'}$), the value of fractional term will be less than 1. Since s_{ip} and $s_{i'p}$ are binary variable, both can not take value of 1. Therefore, channel set p is not assigned to both UAVs i and i' at the same time. Channel sets assigned to at least one candidate point are labeled as used set under constraint (18c). In addition to minimizing the number of selected candidate points, we can reduce the number of used channels by adding term $\sum_{p\in P} e_p$ to the objective function. Assigning exactly one channel set to each selected candidate point is ensured by lowering the number of used channel sets and constraint (18a).

IV. Decision Variable Evaluation in Stochastic Constraint

As we previously indicated, constraints (8) and (9) include uncertain parameter ξ that represents the propagation mode. In this paper, we assume that radio signals emitted by the BSs are line-of-sight (LoS) or non-line-of-sight (NLoS) groups. Depending on the propagation mode, a communication link may have different path losses. The main question that arises due to the uncertainty in ξ is what attributes x_{ij}s and y_js must have to fulfill (8) and (9).

To find properties of advantageous decision x for a stochastic constraint $A(\xi)x - b(\xi) \geq 0$, a quantitative meaning to the term "advantage" should be attached. As $\zeta(x,\xi) = A(\xi)x - b(\xi)$ is a random variable for a given x, a function ρ for evaluating random variables must be chosen first. Based on the definition of ρ, decision vector x will be evaluated as follows:

$$V(x) = \rho(\zeta(x,\xi)).$$

Depending on the interpretation of $\rho(v)$ as either expressing opportunity or risk, "advantageous" will mean that higher or lower values of $\rho(\zeta(x,\xi))$ are considered as preferable, respectively [34]. Below, we introduce the three most commonly used techniques for evaluating decision variables within constraints containing random parameters.

A. Expected value evaluation function

Taking expectation is the easiest technique to assign a quality measure to $\zeta(x,\xi)$. Assuming the existence of the expected values of $A(\xi)$ and $b(\xi)$, expected value evaluation function $\rho_{\mathbb{E}}(v) := \mathbb{E}[v]$ leads to the following formulation of stochastic constraint $A(\xi)x - b(\xi) \geq 0$:

$$\overline{A(\xi)}x - \overline{b(\xi)} \geq 0,$$

where $\overline{A(\xi)}$ and $\overline{b(\xi)}$ are expected value of random vector $A(\xi)$ and random parameter $b(\xi)$ respectively. Constraints (8) and (9) can be expressed as follows using expected value evaluation functions:

$$\begin{aligned}&(\eta_{LoS} - \eta_{NLoS})\mathbb{P}_{ij}[\xi = LoS] + \eta_{NLoS} + FSPL_{ij} \leq \\ &p_t^{(dB)} - p_n^{(dB)} - \frac{1}{0.332}\frac{DR_j}{\beta} + (1 - x_{ij})M \quad \forall i \in I, \quad \forall j \in J\end{aligned} \tag{19}$$

$$\begin{aligned}&(\eta_{LoS} - \eta_{NLoS})\mathbb{P}_{Tj}[\xi = LoS] + \eta_{NLoS} + FSPL_{Tj} \leq \\ &p_T^{(dB)} - p_n^{(dB)} - \frac{1}{0.332}\frac{DR_j}{\beta} + (1 - y_j)M \quad \forall j \in J\end{aligned} \tag{20}$$

As the LoS propagation probability distribution and path loss for user j are functions of the UAV altitude in A2G links, constraint (19) is nonlinear in terms of decision variable h_i.

B. Worst case evaluation function

This approach is based on Madansky's idea [35] who suggested a worst-case approach by prescribing the stochastic constraint for all $\xi \in \Xi$, with Ξ denoting the support of the random vector ξ. The approach corresponds to one of the following choices of the evaluation function:

$$\rho(v) = min_{\hat{v}\in\Theta} min_{1\leq i\leq S} \hat{v}_i,$$
$$\rho(v) = max_{\hat{v}\in\Theta} max_{1\leq i\leq S} \hat{v}_i,$$

where Θ is the support of random variable v and S is the dimension of random vector v. The worst case is indicated by the *min* and *max* functions in these evaluators, which can be adjusted based on the modeling strategy.

In constraints (8) and (9), the random parameter is the propagation model. So we have $S = 1$ and $\Xi = \{LoS, NLoS\}$. Satisfying these constraints for all $\xi \in \Xi$ is equivalent to adding the following constraints to the mathematical model:

$$\begin{aligned}\eta_\xi + FSPL_{ij} \leq p_t^{(dB)} - p_n^{(dB)} - \frac{1}{0.332}\frac{DR_j}{\beta} + (1 - x_{ij})M \\ \forall i \in I, \forall j \in J, \forall \xi \in \Xi,\end{aligned} \tag{21}$$

$$\begin{aligned}\eta_\xi + FSPL_{Tj} \leq p_T^{(dB)} - p_n^{(dB)} - \frac{1}{0.332}\frac{DR_j}{\beta} + (1 - y_j)M \\ \forall j \in J, \forall \xi \in \Xi.\end{aligned} \tag{22}$$

Since $\eta_{NLoS} > \eta_{LoS}$, satisfication of constraints for $\xi = NLoS$ ensures that the constraint for $\xi = LoS$ is met. The NLoS scenario's crucial role in (21) and (22) confirms that NLoS is the worst-case propagation mode. In this strategy, the constraints relating to the control of path loss are linear in terms of decision variables if the BS is terrestrial and nonlinear in the case of UAV-BSs.

C. Chance Constrained Modeling

Major problems with the previous evaluators is that they collapse the entire probability distribution of the uncertain parameter to a one-point (expected value or worst case) while the realization of the random variables, in reality, might not correspond to these values and good decisions may not be investigated due to some realizations of ξ with a low probability of occurance. In the Chance Constrained strategy, x is considered as a feasible solution if it meets stochastic constraints for all $\xi \in S \subset \Xi$. S can be a subset of Ξ with a prescribed probability level. The evaluator in such a case is:

$$\rho_{\mathbb{P}}(v) = \mathbb{P}(v \geq 0)$$

The quality measure of x for constraint $A(\xi)x - b(\xi) \geq 0$ is defined as follows:

$$V(x) = \rho_{\mathbb{P}}(A(\xi)x - b(\xi)) = \mathbb{P}(A(\xi)x - b(\xi) \geq 0)$$

Taking constraints of the form $V(x) \geq \delta$, with δ being a high probability level, we have:

$$\mathbb{P}(A(\xi)x - b(\xi) \geq 0) \geq \delta$$

Using chance constraints, (8) and (9) can be reformulated as follows:

$$\mathbb{P}_{\xi}[PL_{ij}^{\xi} \leq p_t^{(dB)} - p_n^{(dB)} - \frac{1}{0.332}\frac{DR_j}{\beta} + (1 - x_{ij})M] \geq \delta \quad (23)$$

$$\mathbb{P}_{\xi}[PL_{Tj}^{\xi} \leq p_T^{(dB)} - p_n^{(dB)} - \frac{1}{0.332}\frac{DR_j}{\beta} + (1 - y_j)M] \geq \delta \quad (24)$$

Proposition 1. *To satisfy constraint* (23) *for user j and candidate point i, the decision variable x_{ij} can be set to 1 only if either the path loss in NLoS propagation does not exceed $PL_{max}^{j} = p_t^{(dB)} - p_n^{(dB)} - \frac{1}{0.332}\frac{DR_j}{\beta}$ or $PL_{ij}^{LoS} = \eta_{LoS} + FSPL_{ij} < PL_{max}^{j} < PL_{ij}^{NLoS} = \eta_{NLoS} + FSPL_{ij}$ while $\mathbb{P}_{ij}[\xi = LoS] \geq \delta$.*

Proof. As mentioned before, we considered two realizations for ξ, $\Xi = \{LoS, NLoS\}$. So, PL_{ij}^{ξ} can be PL_{ij}^{LoS} or PL_{ij}^{NLoS}. Since $PL_{ij}^{LoS} < PL_{ij}^{NLoS}$ for $i \in I$ and $j \in J$, one of the following four situations occurs:

1) $PL_{max}^{j} < PL_{ij}^{LoS} < PL_{ij}^{NLoS}$
2) $PL_{ij}^{LoS} \leq PL_{max}^{j} < PL_{ij}^{NLoS}$ and $\mathbb{P}_{ij}[\xi = LoS] < \delta$
3) $PL_{ij}^{LoS} \leq PL_{max}^{j} < PL_{ij}^{NLoS}$ and $\mathbb{P}_{ij}[\xi = LoS] \geq \delta$
4) $PL_{ij}^{LoS} < PL_{ij}^{NLoS} \leq PL_{max}^{j}$

In the first case, if x_{ij} takes value 1, constraint (8) is violated with a probability of 1 . So, x_{ij} must be 0. If x_{ij} is 1 in the second case, the path loss is less than PL_{max}^{j} only if the propagation is *LoS*. x_{ij} must also be 0 for the second case since the probability of *LoS* propagation is less than δ. In the third case, constraint (8) will be satisfied with a probability greater than δ if x_{ij} takes value 1. Therefore, in this case, the path loss bound can not prevent x_{ij} from becoming 1. In last case, even if *NLoS* propagation occurs and x_{ij} is set to 1, the path loss will not greater than PL_{max}^{j}. To summarize, x_{ij} must take value according to the following conditional expression to satisfy constraint (23).

$$x_{ij} = \begin{cases} 0 & \text{if } PL_{max}^{j} < PL_{ij}^{LoS} < PL_{ij}^{NLoS} \\ 0 & \text{if } PL_{ij}^{LoS} \leq PL_{max}^{j} < PL_{ij}^{NLoS} \& \mathbb{P}_{ij}[\xi = LoS] < \delta \\ 0 \text{ or } 1 & \text{if } PL_{ij}^{LoS} \leq PL_{max}^{j} < PL_{ij}^{NLoS} \& \mathbb{P}_{ij}[\xi = LoS] \geq \delta \\ 0 \text{ or } 1 & \text{if } PL_{ij}^{LoS} < PL_{ij}^{NLoS} \leq PL_{max}^{j} \end{cases} \quad (25)$$

We reformulate constraint (23) or equivalently (25) as follows:

$$PL_{max}^{j} \geq \eta_{LoS} + FSPL_{ij} - (1 - x_{ij})M \quad \forall i \in I, j \in J, \quad (26a)$$

$$PL_{max}^{j} \geq \eta_{NLoS} + FSPL_{ij} - (1 - w_{ij})M \quad \forall i \in I, j \in J, \quad (26b)$$

$$\mathbb{P}_{ij}[\xi = LoS] \geq \delta - 2(1 - \gamma_{ij}) \quad \forall i \in I, j \in J, \quad (26c)$$

$$x_{ij} \leq w_{ij} + \gamma_{ij} \quad \forall i \in I, j \in J, \quad (26d)$$

Constraint (26a)-(26d) value decision variables w_{ij} and γ_{ij} as follows:

$$w_{ij} = \begin{cases} 0 & \text{if } PL_{max} < \eta_{NLoS} + FSPL_{ij} \\ 0 \text{ or } 1 & \text{otherwise} \end{cases}$$

$$\gamma_{ij} = \begin{cases} 0 & \text{if } \mathbb{P}_{ij}[\xi = LoS] < \delta \\ 0 \text{ or } 1 & \text{otherwise} \end{cases}$$

According to constraint (26a), if $PL_{j}^{max} < PL_{ij}^{LoS}$, decision variable x_{ij} takes value of 0. In constraints (26b), variable w_{ij} must take zero value if $PL_{ij}^{NLoS} < PL_{j}^{max}$. Also constraint (26c) makes γ_{ij} zero if $\mathbb{P}_{ij}[\xi = LoS] < \delta$. Constraint (26d) states that x_{ij} will be zero if both w_{ij} and γ_{ij} are zero. To control the path loss between the user j and the terrestrial BS, constraints (26a)-(26d) are repeated for $i = 0$.

V. Linearization of Nonlinear Constraints

Constraints (19), (21), and (26a)-(26c) are nonlinear in terms of decision variables due to the nonlinear relation between $FSPL_{ij}$ and probability of *LoS* communication with the altitude of the UAV. Linearization of these functions leads to a linear formulation in terms of decision variables. This provides the chance to use accurate solving algorithms for MIPs such as branch and bound (B & B) as well as powerful solvers such as CPLEX that exploit these algorithms. In this study, we use piecewise linear approximation of path loss and LoS probability distribution functions to improve accuracy. A comparison of linear and piecewise linear approximations of these functions for a user in an urban setting who is 100 meters from a candidate point is shown in Figures 2 and 3.

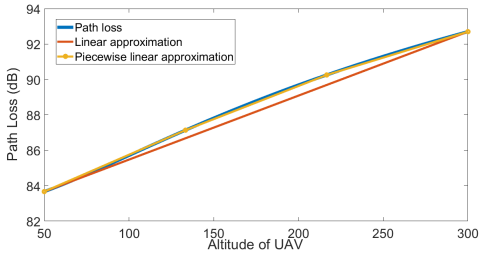

Fig. 2: Path loss approximations

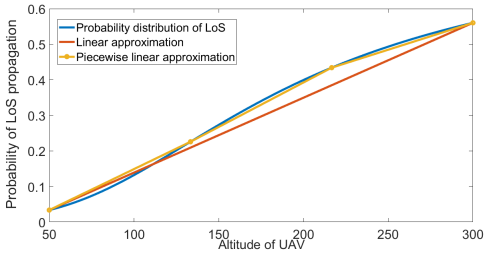

Fig. 3: LoS probability distribution approximations

In utilizing piecewise linear approximations, we need to know the altitude of the UAV so that the corresponding line can be selected. However, the UAV altitude is a decision variable and doesn't take value before the model is solved. Accordingly, the mathematical model must be able to determine the correct line based on the altitude of the UAV. We use the following lemma to obtain the values of $FSPL_{ij}$ and $\mathbb{P}_{ij}[\xi = LoS]$ by determining the containing interval of the UAV altitude.

Lemma 2. *Suppose that $H_1 < H_2 < \cdots < H_k$ and continious piecewise linear function $f(h)$ is defined on $[H_1, H_k]$ and is known at points $(H_i, f(H_i))$. Each $h \in [H_1, H_k]$ has a representation in form of $\sum_{i=1}^{k} \lambda_i H_i$, in which the λ_is are non-negative numbers with a sum of 1. This representation is unique if at most two consecutive coefficients are non-zero. Moreover, we have:*

$$f(h) = \sum_{i=1}^{k} \lambda_i f(H_i).$$

Now, suppose that the altitude range is partitioned as follows:

$$[H_{min}, H_{max}] = [H_1 = H_{min}, H_2, \ldots, H_{K-1} = H_{max}, H_K = H_{max} + \Delta]$$

where $\Delta > 0$. Also, assume that the values of $FSPL_{ij}$ and LoS probability functions are given by L_{ijk} and pr_{ijk} for user j, candidate point i, and a UAV deployed at the altitude of H_k. We develop the mathematical model such that the h_i variables for unselected candidate points takes a value of H_K. In order to obtain the correct values of the piecewise linear approximations of $FSPL_{ij}$ and $\mathbb{P}_{ij}[\xi = LoS$ in terms of the altitude of UAV deployed at candidate point i, the following constraints are added to the mathematical model:

$$h_i = \sum_{k=1}^{K} \lambda_{ik} H_k \quad \forall i \in I \tag{27a}$$

$$n_{ij} = \sum_{k=1}^{K} \lambda_{ik} L_{ijk} \quad \forall i \in I, \quad \forall j \in J \tag{27b}$$

$$o_{ij} = \sum_{k=1}^{K} \lambda_{ik} pr_{ijk} \quad \forall i \in I, \quad \forall j \in J \tag{27c}$$

$$\sum_{k=1}^{K-1} \lambda_{ik} + (1 - m_i) = 1 \quad \forall i \in I \tag{27d}$$

$$\lambda_{i1} \leq g_{i1} \quad \forall i \in I \tag{27e}$$

$$\lambda_{ik} \leq g_{ik-1} + g_{ik} \quad \forall i \in I, \quad \forall k \in 2, \ldots, K-1 \tag{27f}$$

$$\lambda_{iK} \leq g_{iK-1} \quad \forall i \in I \tag{27g}$$

$$\sum_{k=1}^{K-1} g_{ik} = 1 \forall i \in I \tag{27h}$$

By applying the constraints (27a) - (27c) we calculate the free space path loss between user j and UAV i as well as the probability of LoS communication, which we denote by decision variables n_{ij} and o_{ij} respectively. Constraint (27d) values the λ variables associated with the UAV altitude. If candidate point i is selected $(m_i = 1)$, $\sum_{k=1}^{K-1} \lambda_{ik}$ must be 1. Otherwise, $\sum_{k=1}^{K-1} \lambda_{ik}$ is zero, if candidate point i is not chosen by the model $(m_i = 0)$. Based on the constraints (27e) - (27h), at most two consecutive λ coefficients can be non-zero, where g_{ik} is a binary decision variable with the following definition:

$$g_{ik} = \begin{cases} 1 & \text{if } H_k \leq h_i < H_{k+1} \\ 0 & \text{otherwise} \end{cases}$$

A linear model is achieved by replacing $FSPL_{ij}$ and $\mathbb{P}_{ij}[\xi = LoS]$ in nonlinear constraints with n_{ij} and o_{ij} respectively. The formulation presented is a mixed binary linear programming (MBLP) and powerful solvers such as CPLEX are available for accurate solving. However, according to the complexity theory, the complexity of mathematical models is an exponential function of decision variables numbers and constraints [36]. This denotes that slight modifications in these factors may have a noteworthy effect on the solving time. So, for this particular formulation, an increase in user and candidate point numbers may result in an unacceptable solving time. The next section presents a decomposition of the integrated model of UAV placement, user association, and channel allocation in which the total number of variables and constraints of its sub-models is considerably fewer than the master model.

VI. MODEL DECOMPOSITION

As the primary objective of this paper is to minimize the number of UAVs needed to meet user demand, our suggested method consists of two steps, the first for minimizing the number of UAVs, and the second for minimizing the number of channel sets. In the first step, a model consist of primary UAV placement, user association, and linearization constraints is used to determine the deployment points and assign users to the BSs:

$$\min \sum_{i \in I} m_i$$

s.t

(1b) – (1i)

(19) – (20) → If the Expected Value strategy is adopted

(21) – (22) → If the Worst Case strategy is adopted

(26a) – (26d) → If the Chance Constrained strategy is adopted

(27a) – (27h)

The second step model allocates radio resources to the UAVs using channel allocation constraints. In the first step, interference avoidance considerations are not taken into account. So, its optimal solution does not necessarily obtain the lowest possible altitude of the UAVs. In the second step, to minimize inter-cell interference, we reduce the altitudes to the extent that it does not violate providing the data rate required by the users (which has been met in the first step). In other words, only the candidate points selected $(\{i | m_i = 1\})$ and the established linkes $(\{(i, j) | x_{ij} = 1\})$ in the previous step are included in the following mathematical model:

$$\min \sum_{p \in P} e_p$$

s.t

(18a) – (18c)

(19) → If the Expected Value strategy is adopted

(21) → If the Worst Case strategy is adopted

(26b) – (26d) → If the Chance Constrained strategy is adopted

(27a) – (27h)

By discarding unselected candidate points and unestablished links, a significant number of decision variables $(x_{ij}, s_{ip}, h_i, w_{ij}, \gamma_{ij}, n_{ij}, o_{ij}, \lambda_{ik}, g_{ik})$ as well as many constraints that were formulated for each candidate point and user during channel allocation calculations are eliminated which ultimately leads to a decrease in solving time.

VII. NUMERICAL RESULTS

In this Section, we first introduce the test system and simulation parameters. Then, a comparison is made between

the results obtained by stochastic approaches suggested in this paper and those obtained by implementing the deterministic method presented in [33].

A. Test system

Our simulations consider only one owner and centralized decision-making for the network provider. We consider a 4000×4000 meter area with scenarios including 200 and 400 users in three different environmental settings: dense urban, urban, and suburban zones. In dense urban environments, 80% of users' positions are generated using Poisson Point Process in groups of 30-40 users. The remained users' position follows a uniform distribution. These percentages are reduced in urban and suburban areas, falling to 50 and 20 respectively. Also, each dense category's user numbers drop to 25 and 10, respectively. The candidate point set is generated by the MergeCells algorithm presented in [33]. A quality constraint requires that at least α percent of users be covered. We consider three different values for α , specically 50, 70, and 90%. In addition, the implementations are performed for six values of δ (Chance Constraint parameter or probability of satisfying path loss constraint) including 70, 80, 90, 95, 97, and 99%. The data rate required by each user has a value between 3 to 10 Mbps with a uniform distribution. Each UAV is assumed to have a backhaul data rate of 450 Mbps, which is the maximum sum of uplink rates for covered users. UAV flying altitude is between 50 and 250 meters. We also consider an elevation angle of 45 degrees, so the coverage radius would be the same as the altitude. Table IV illustrates parameter values for each scenario.

TABLE IV: Test parameters.

Parameter	Value
Carrier frequency (f_c)	2.5 GHz
Speed of light (C)	$3 \times 10^8 m/sec$
Number of users (U)	200,400
GBS data rate (D_T)	1000
GBS coverage radius (R_T)	400m
UAV data rate (D)	450 Mbps
UAV altitude range ($[H_{min}, H_{max}]$)	[50,250]
UAV elevation angle (θ)	45, 60 degree
Coverage percentage (α)	50, 70,and 90%
Chance constraint parameter (δ)	70, 80, 90, 95, 97, and 99%
Propagation critical distances (k_0, k_1)	80, 164
Enviromental setting [37]	$(a, b, \eta_{LoS}, \eta_{NLoS})$
Dense	(12.08,0.11,$10\log_{10}1$, $10log_{10}20$)
Urban	(9.61,0.19,$10\log_{10}1$, $10log_{10}20$)
Suburban	(4.88,0.43,$10\log_{10}0.1$, $10log_{10}21$)

To have informative and generalizable results in the rest of our simulations we present results that are the average of 50 runs for each scenario. CPLEX Studio IDE is used for solving the proposed mathematical model on a system with 32 GB RAM and 2.4 GHz Core-i7 CPU.

B. Result

In the following, we compare the results of the approaches presented in this paper with the deterministic method proposed in [33]. For deterministic method, the maximum allowable path loss of the links must be specified. We calculate this value using the maximum required data rate of users in a LoS configuration.

The worst case and Chance Constrained method with $\delta = 0.99$ are removed from comparisons in this study due to the infeasibility of associated models. However, these methods might fulfill the path loss constraints by selecting a large number of points from a bigger set than the candidate points generated by MergeCells method. In Figure 4, an overview of the average number of UAVs required in different instances of each scenario is reported. Figure 4 shows that despite the lack of guarantee in meeting the path loss constraint, deterministic strategy uses a relatively high number of UAVs. Although it was expected that the deterministic method's consideration of a free space environment would result in fewer UAVs, a path loss bound based only on LoS propagation makes stricter limits and increases the required number of UAVs. According to Figure 4, the number of UAVs required increases with the number of users and the desired coverage percentage. Furthermore, in the deterministic method, the number of UAV-BSs is an increasing function of the scattering of users in the target area. However, in stochastic methods, where propagation mode uncertainty is considered, the urban environment has the highest average number of UAVs. This result may be explained by the fact that in densely populated areas, where users are closer together, a UAV can cover more users per flight. Suburban areas are also more likely to have LoS communications and lower path loss values due to fewer obstacles. Therefore, stochastic methods provide a better diagnosis of factors affecting the number of UAV-BSs required. Figure 4 indicates that with an increase in the δ value (resulting in a decrease in the risk of violating the path loss constraint), the number of UAVs required increases. Figure 4 has also provided a deeper insight into the number of UAVs for the Chance Constrained method. In these methods, as population density is reduced, changes in δ result in fewer changes in the number of UAVs. The reason is that the inverse relation between population density and obstacles with the chance of LoS communication increases the probability of meeting the path loss constraint in scattered environments. Although the methods that utilize more UAVs are able to provide more data rates, they are less concerned with meeting the network requirements with the least number of UAVs. In the following we provide an analysis of how different deployments satisfy data rate requirements. For this purpose, we define the efficiency index inspired by the Goal programming to measure overachieving and underachieving levels of the data rate requirements.

$$\text{Efficiency index} = \frac{\text{Potential data rate} - \text{Required data rate}}{\text{Required data rate}}, \quad (28)$$

where

$$\text{Potential data rate} = \frac{\sum_{i\in I}\sum_{j\in I|x_{ij}=1} 0.332 \times snr_j \times \beta_{min}}{\sum_{i\in I} m_i},$$
$$\text{Required data rate} = \frac{\sum_{i\in I}\sum_{j\in I|x_{ij}=1} DR_j}{\sum_{i\in I} m_i}. \quad (29)$$

In other words, the efficiency index is the relative deviation from the required data rate of the network. Negative values for this index indicate the inefficiency of the method in meeting the network's needs. Furthermore, a deployment whose performance index approaches zero is more acceptable. In Figure 5 different methods are compared in terms of their efficiency in different scenarios for 400 users. The results shows that stochastic methods, particularly Chance Constrained ones, outperform the deterministic approach significantly.

Besides the position of a UAV-BS, its elevation angle also influences the total data rate that it can offer. A higher elevation angle implies a wider coverage area for a UAV-BS. We investigate how varying this angle affects the system performance by comparing the average number of users served by each UAV-BS in two modes of the elevation angle in Figure 6. Figure 6 shows that as the elevation angle grows, expanding the coverage area leads to an increase in the average number of users that each UAV can serve. However, the rate of increase slows down as the δ increases in Chance Constrained strategy. This is because although the coverage area increases as the θ grows, the users at the cell edge will experience

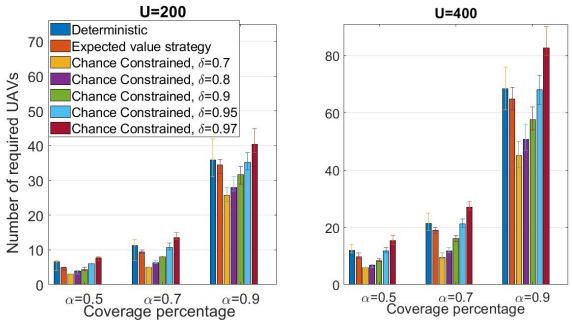

(a) Dense environment.

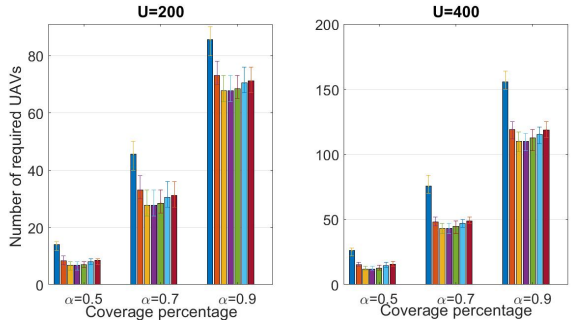

(b) Urban environment.

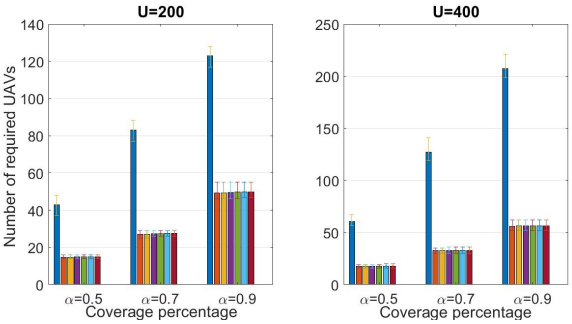

(c) Suburban environment.

Fig. 4: Number of UAVs, $\theta = 45$.

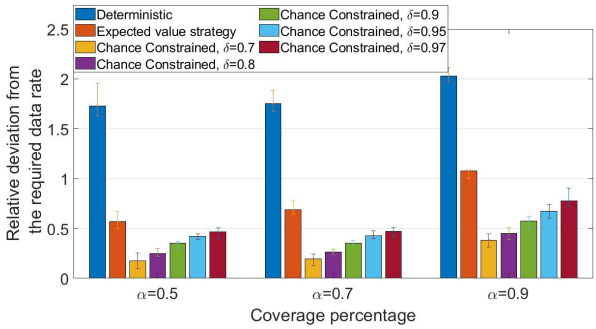

(a) Dense environment.

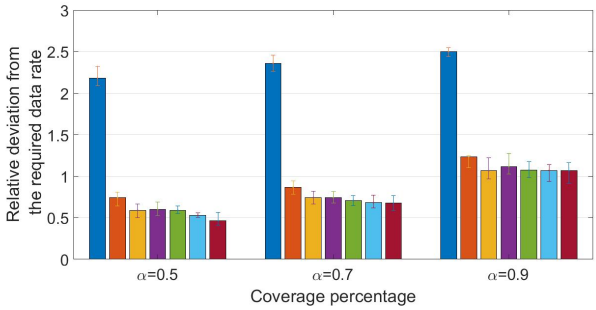

(b) Urban environment.

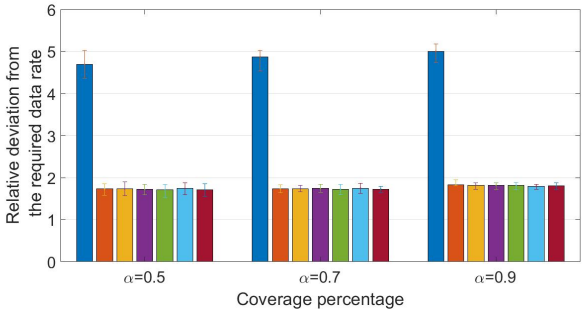

(c) Suburban environment.

Fig. 5: Efficiency index of deployments, $U = 400$, $\theta = 45$.

LoS communication with a lower probability. Therefore, to meet the path loss constraint for larger values of δ, the model decides to deploy more UAVs. Figure 6 also shows that as the users become denser in the target area, the improvement in the average number of users covered by each UAV decreases. The explanation is that in denser scenarios, the constraint on the maximum number of users that each UAV-BS can serve becomes more influential.

As described in section IV, the proposed stochastic methods use the probability distribution of the random parameters to make decisions on UAV deployment and user association. However, the values of random parameters are realized after the decision-making process. In such a situation, what is important is how these methods perform when the random parameters are realized. For example, the Chance Constraint method guarantees a lower bound (δ) for the probability of satisfying path loss constraint. But how is compliance with this guarantee measured? To examine the performance of each method in different realizations of random parameters, we use Monte Carlo simulation. In this way, we generate 2000 random states for each link propagating mode based on the probability distribution functions (14) and (16). By calculating the path loss of each link in the generated configuration, the number of links that violate path loss constraints is determined. Figure 7 shows the ratio of the number of violated constraints to the total configurations generated. According to Figure 7, the deterministic method never violates the allowable path loss due to the hard constraint on the path loss bound and utilizing more UAVs. However, in stochastic approaches, this rate reaches a maximum of 0.09.

Using a large number of UAVs not only misses the primary objective of minimizing the required UAV-BSs but also poses a higher risk of inter-cell interference. Minimizing the number of UAVs makes them to fly at a higher altitude to achieve the desired coverage percentage. Flying at a higher level enlarges the UAVs' coverage area and increases overlap probability. After determining the minimum number of UAVs in the first step of the proposed method, the second stage improves the UAVs' altitude to minimize inter-cell interference between UAV-BSs. Figure 8 illustrates the areas that are covered by each base station and the overlapping regions. The orange circle represents the coverage area of the terrestrial base station while the other circles indicate the coverage areas of the UAVs. UAV-BSs that have identical coverage area colors can utilize

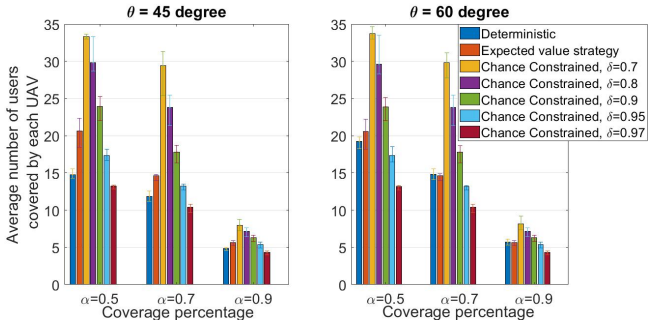

(a) Dense environment.

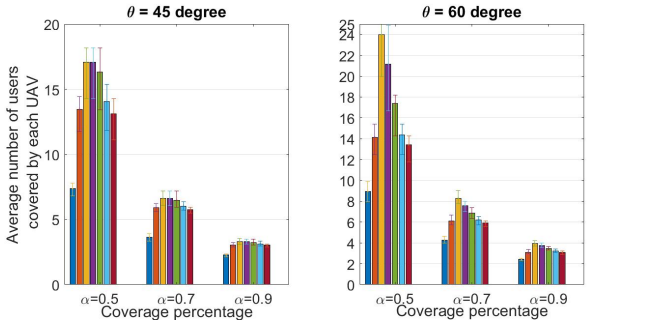

(b) Urban environment.

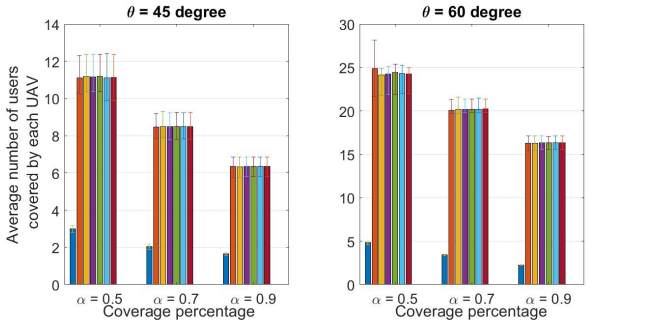

(c) Suburban environment.

Fig. 6: average number of users covered by each UAV, $U = 400$.

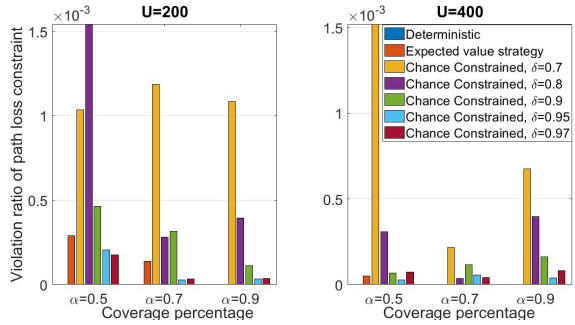

(a) Dense environment.

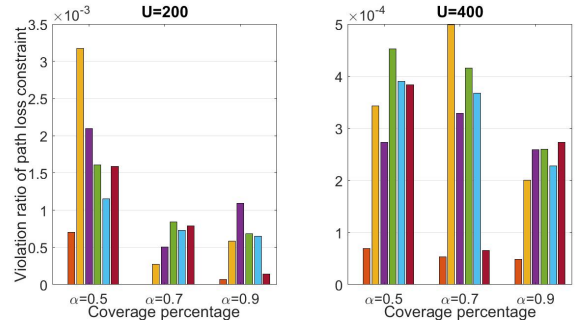

(b) Urban environment.

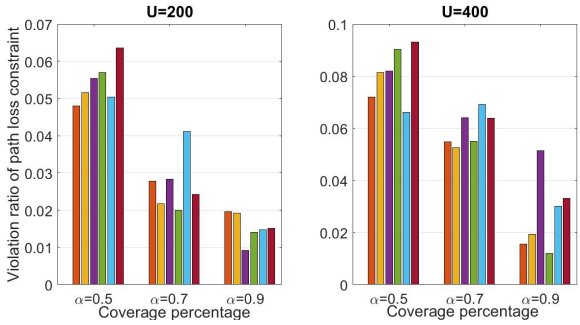

(c) Suburban environment.

Fig. 7: Monte Carlo simulation, $\theta = 45$.

the same channel sets. Figure 8 shows the reduction in the overlapped coverage areas by improving UAV altitudes for a scenario of 400 users, in a suburban environment. The number of channel sets to prevent inter-cell interference is three in the first stage deployment (Figure 8a), while it is downsized to two in the second phase (Figure 8b).

Minimizing distinct channel sets required, resulting in more bandwidth being allocated to each set in the bandwidth division. Increasing bandwidth for each channel set will lead to an increase in SNR, a reduction in path loss, and a greater chance of satisfying needed data rate. Figure 9 illustrates the minimum number of channel sets required to serve 90% of 400 users in different environments. According to Figure 9, densely populated environments necessitate a greater number of distinct channel sets. So, interference is more likely to occur in dense urban environments if the optimal resource allocation considerations are not followed. Figure 9 also illustrates how the number and altitude of UAVs affect the number of distinct channel sets required. The opposing behavior of the UAV number and average altitude graphs shows the admissible performance of the methods in interference control. A low number of UAVs result in a higher average altitude to ensure the desired coverage while more UAV-BSs lead to lower altitudes with the aim of avoiding interference. According to Figure 9, the number of UAV-BSs is more influential on interference than the UAVs' average altitude in dense urban environments. However, in suburban areas, the altitude of UAVs plays a significant role in interference. In an urban environment, the number of required channel sets for interference avoidance is affected simultaneously by the number and altitude of UAVs.

In terms of complexity, the solving time of the integrated mathematical model surpasses the 500-seconds limit applied to CPLEX and is not practical for real scenarios. Therefore, as stated earlier, we use a decomposed model as an effective approach to ensure practicality and feasibility. A comparison of the methods mentioned in this paper can be found in Figure 10. According to Figure 10, stochastic approaches, particularly Chance Constrained methods, need only a maximum of 30 seconds more time than the deterministic optimization.

One other common way of assessing the complexity of decomposition method is to examine how the computing time increases as the problem size grows [38]. In this paper, the computational complexity of each approach is directly related

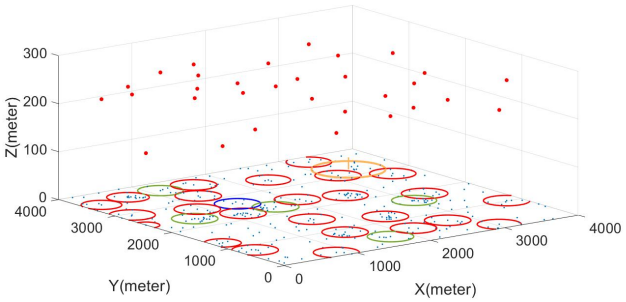

(a) First stage deployment.

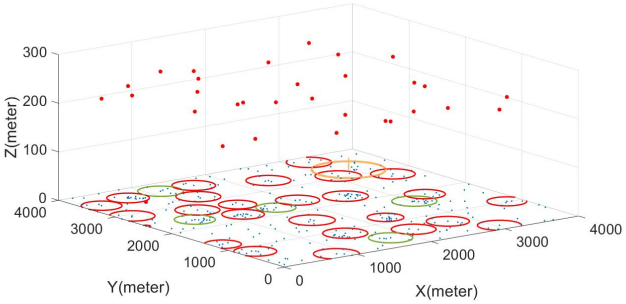

(b) Second stage deployment.

Fig. 8: Improving altitude of UAVs, $\alpha = 0.7, U = 400$, $\theta = 45$, Chance Constrained, $\delta = 0.95$.

to the size of mathematical models that must be solved, which can be roughly measured by the number of variables and constraints within the first- and second-stage models.

TABLE V: The number of variables and constraints in the first-stage model

	Variables	Constraint (1b) -(1i)	Stochastic constraints	Constraint (27a) -(27h)
Worst Case	$I(3J+2K+3)$	$IJ+4I+J+2$	$J(I+1)$	$I(2J+K+5)$
Expected value	$I(3J+2K+3)$	$IJ+4I+J+2$	$J(I+1)$	$I(2J+K+5)$
Chance Constrained	$I(5J+2K+3)$	$IJ+4I+J+2$	$4J(I+1)$	$I(2J+K+5)$

Since the constraints of the second-stage model are created based on the candidate point selection and the user association obtained from the first stage, their enumeration will be as follows:

TABLE VI: The number of constraints in the second-stage model

	Constraint (18a) -(18c)	Stochastic constraints	Constraint (27a) -(27h)
Worst Case	$(I^{'2}-I^{'}+1)P+I^{'}$	J	$6I^{'}+2J$
Expected value	$(I^{'2}-I^{'}+1)P+I^{'}$	J	$6I^{'}+2J$
Chance Constrained	$(I^{'2}-I^{'}+1)P+I^{'}$	$4J$	$6I^{'}+2J$

where $I^{'}$ is the number of selected candidate points and J is the number of users or the maximum number of established links. As shown in Table V and VI, the determining factors for the size of the presented models are the number of users ($|J|$) and candidate points ($|I|$) as well as the accuracy of the piecewise linear approximation and the maximum number of channel sets (P).Therefore, increasing the number of users or the environment size will lead to a growth in computational complexity due to the increased parameters I and J. Also, Table V and VI indicate that the Chance Constrained models

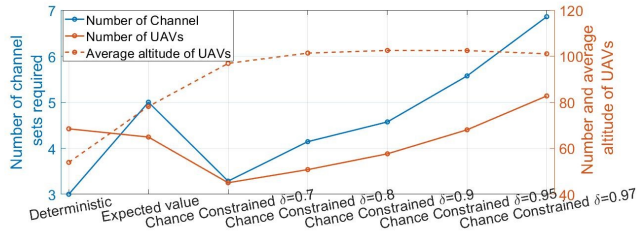

(a) Dense environment.

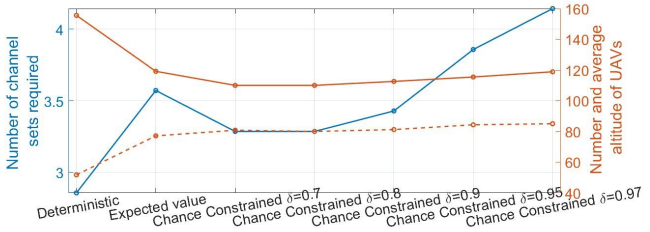

(b) Urban environment.

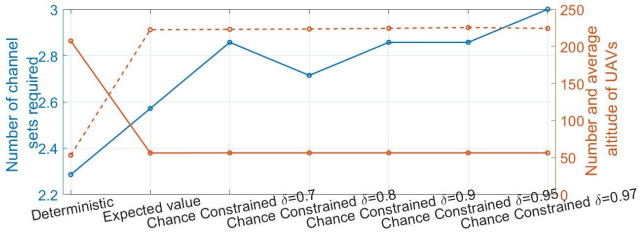

(c) Suburban environment.

Fig. 9: The effects of UAV number and average altitude on resource allocation, $\alpha = 0.9, U = 400, \theta = 45$.

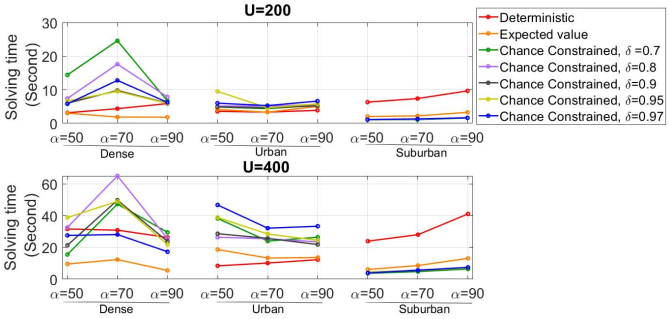

Fig. 10: Average solving time, $\theta = 45$.

involve more variables and stochastic constraints than the worst-case and expected value approaches. So, it is anticipated that the maximum computational time of this strategy will be higher than the other two methods. In exchange for the higher computational complexity, as demonstrated so far, the solution obtained from the Chance Constrained strategy has a better performance and a more accurate discernment of the uncertain environment. Moreover, this method is able to satisfy the specified guarantee for meeting the stochastic constraints.

VIII. Conclusion

The purpose of the current study was to determine the most cost-effective integration of UAVs into a wireless network that satisfies the users' requirements. It was, therefore, necessary to

design a deployment strategy to minimize the number of UAVs while meeting the minimum data rate required by the users as a lower bound on service level. This paper accounted for factors including users' distance to the BS, the density of the area, the environmental setting, and the resource allocation technique to achieve a realistic and practical deployment of UAVs. Since these factors randomly affect the achievable data rate received by the users, three common ways of modeling uncertainty have been customized to analyze the deployment requirements: 1) Expected value strategy, 2) Worst case, and 3) Chance Constrained. Mathematical models were developed for each case and linearized utilizing piecewise linear approximations of the path loss and probability of LoS functions. Models were solved in a practical time by decomposing them into two stages, where a minimum number of UAVs is found in the first stage.A frequency reuse strategy for resources allocation, and an improvement of UAV placement are determined in the second step. The stochastic methods in this study appear to provide a more detailed analysis of the uncertainty involved in the UAV deployment problem than deterministic method presented in [33]. Furthermore, solutions obtained by these models are significantly more efficient than those obtained by the deterministic method.

REFERENCES

[1] Tam, Ho Huu Minh, et al. "Joint load balancing and interference management for small-cell heterogeneous networks with limited backhaul capacity." *IEEE Transactions on Wireless Communications* 16.2 (2016): 872-884.

[2] Kalantari, Elham, et al. "On the number and 3D placement of drone base stations in wireless cellular networks." *2016 IEEE 84th Vehicular Technology Conference (VTC-Fall).* IEEE, 2016.

[3] Mozaffari, Mohammad, et al. "A tutorial on UAVs for wireless networks: Applications, challenges, and open problems." *IEEE communications surveys & tutorials* 21.3 (2019): 2334-2360.

[4] Qiu, Chen, et al. "Multiple UAV-mounted base station placement and user association with joint fronthaul and backhaul optimization." *IEEE Transactions on Communications* 68.9 (2020): 5864-5877.

[5] Shakoor, Shanza, et al. "Joint optimization of UAV 3-D placement and path-loss factor for energy-efficient maximal coverage." *IEEE Internet of Things Journal* 8.12 (2020): 9776-9786.

[6] Mozaffari, Mohammad, et al. "Efficient deployment of multiple unmanned aerial vehicles for optimal wireless coverage." *IEEE Communications Letters* 20.8 (2016): 1647-1650.

[7] Sobouti, Mohammad Javad, et al. "Efficient deployment of small cell base stations mounted on unmanned aerial vehicles for the internet of things infrastructure." *IEEE Sensors Journal* 20.13 (2020): 7460-7471.

[8] Alzenad, Mohamed, et al. "3-D placement of an unmanned aerial vehicle base station for maximum coverage of users with different QoS requirements." *IEEE Wireless Communications Letters* 7.1 (2017): 38-41.

[9] Alzenad, Mohamed, et al. "3-D placement of an unmanned aerial vehicle base station (UAV-BS) for energy-efficient maximal coverage." *IEEE Wireless Communications Letters* 6.4 (2017): 434-437.

[10] Cherif, Nesrine, et al. "On the optimal 3D placement of a UAV base station for maximal coverage of UAV users." *GLOBECOM 2020-2020 IEEE Global Communications Conference.* IEEE, 2020.

[11] Zou, Chengming, et al. "3D placement of unmanned aerial vehicles and partially overlapped channel assignment for throughput maximization." *Digital Communications and Networks* 7.2 (2021): 214-222.

[12] S. ur Rahman, Shams, et al. "Positioning of UAVs for throughput maximization in software-defined disaster area UAV communication networks." Journal of Communications and Networks 20.5 (2018): 452-463.

[13] Munaye, Yirga Yayeh, et al. "UAV positioning for throughput maximization using deep learning approaches." Sensors 19.12 (2019): 2775.

[14] Singh, Sandeep Kumar, et al. "On UAV selection and position-based throughput maximization in multi-UAV relaying networks." IEEE Access 8 (2020): 144039-144050.

[15] Mozaffari, Mohammad, et al. "Mobile unmanned aerial vehicles (UAVs) for energy-efficient Internet of Things communications." *IEEE Transactions on Wireless Communications* 16.11 (2017): 7574-7589.

[16] Wang, Lei, Bo Hu, and Shanzhi Chen. "Energy efficient placement of a drone base station for minimum required transmit power." *IEEE Wireless Communications Letters* 9.12 (2018): 2010-2014.

[17] Ghanavi, Rozhina, et al. "Efficient 3D aerial base station placement considering users mobility by reinforcement learning." *2018 IEEE Wireless Communications and Networking Conference (WCNC).* IEEE, 2018.

[18] Mozaffari, Mohammad, et al. "Drone small cells in the clouds: Design, deployment and performance analysis." *2015 IEEE global communications conference (GLOBECOM).* IEEE, 2015.

[19] Khuwaja, Aziz A, et al. "Optimum deployment of multiple UAVs for coverage area maximization in the presence of co-channel interference." *IEEE Access.* 7 (2019): 85203–85212.

[20] Rohde, Sebastian, et al. "Ad hoc self-healing of OFDMA networks using UAV-based relays." *Ad Hoc Networks.* 11.7 (2013): 1893–1906.

[21] Noh, Si-Chan, et al. "Energy-efficient deployment of multiple UAVs using ellipse clustering to establish base stations." *IEEE Wireless Communications Letters.* 9.8 (2020): 1155–1159.

[22] Mozaffari, Mohammad, et al. "Efficient deployment of multiple unmanned aerial vehicles for optimal wireless coverage." *IEEE Communications Letters.* 20.8 (2016): 1647–1650.

[23] Sun, Jingcong and Masouros, Christos "Deployment strategies of multiple aerial BSs for user coverage and power efficiency maximization." *IEEE Transactions on Communications.* 67.4 (2018): 2981–2994.

[24] Liu, Liang, et al "CoMP in the sky: UAV placement and movement optimization for multi-user communications." *IEEE Transactions on Communications.* 67.8 (2019): 5645–5658.

[25] Wang, Chuanan, et al "Joint user association and interference mitigation for drone-assisted heterogeneous wireless networking." *EURASIP Journal on Wireless Communications and Networking.* 2019.1 (2019): 1–8.

[26] Novlan, Thomas David , et al "Analytical evaluation of fractional frequency reuse for OFDMA cellular networks." *IEEE Transactions on wireless communications.* 10.12 (2011): 4294–4305.

[27] Hossain, Md Sakir and Becvar, Zdenek "Flexible soft frequency reuse for interference management in the networks with flying base stations." *2020 IEEE 91st Vehicular Technology Conference (VTC2020-Spring).* (2020): 1–7.

[28] Lee, Seungmin, et al "Optimal Frequency Reuse and Power Control in Multi-UAV Wireless Networks: Hierarchical Multi-Agent Reinforcement Learning Perspective." *IEEE Access.* 10 (2022): 39555–39565.

[29] Nguyen, Minh Dat, et al. "UAV placement and bandwidth allocation for UAV based wireless networks." 2019 IEEE Global Communications Conference (GLOBECOM). IEEE, 2019.

[30] Fontanesi, Gianluca, et al. "Outage analysis for millimeter-wave fronthaul link of UAV-aided wireless networks." *IEEE Access.* 8 (2020): 111693-111706.

[31] Fontanesi, Gianluca, et al. "A transfer learning approach for UAV path design with connectivity outage constraint." *IEEE Internet of Things Journal.* 10.6 (2022): 4998-5012.

[32] Rahimi, Zahra, et al. "3D UAV BS Positioning and Backhaul Management in Cellular Network Via Stochastic Optimization." GLOBECOM 2022-2022 IEEE Global Communications Conference. IEEE, 2022.

[33] Rahimi, Zahra, et al. "An Efficient 3D Positioning Approach to Minimize Required UAVs for IoT Network Coverage." *IEEE Internet of Things Journal* (2021).

[34] Kall, Peter, et al. "Stochastic Linear Programming Models, Theory, and Computation." Springer New York, NY, 2011.

[35] Madansky, Albert. "New Methods in Mathematical Programming-Methods of Solution of Linear Programs Under Uncertainty." Operations Research 10.4 (1962): 463-471.

[36] Sánchez, J. M. García "Modelling in mathematical programming : methodology and techniques" Springer, 2021.

[37] Sekander, Silvia et al. "Multi-tier drone architecture for 5G/B5G cellular networks: Challenges, trends, and prospects." *IEEE Communications Magazine* (2018).

[38] Wolsey, Laurence A., and George L. Nemhauser. "Integer and combinatorial optimization." Vol. 55. John Wiley Sons, 1999.